



# Computer modelling of the ablation casting process and prediction of the strength properties of AC-42000 castings

Marcin Małysza<sup>1,2\*</sup> , Sabina Puzio<sup>2</sup> , Katarzyna Major-Gabryś<sup>2</sup> ,  
Mirosław Głowacki<sup>2</sup> , Dorota Wilk-Kołodziejczyk<sup>1,2</sup> , Jadwiga Kamińska<sup>1</sup> 

<sup>1</sup> Centre of Casting Technology, Łukasiewicz Research Network – Krakow Institute of Technology, Krakow, Poland.

<sup>2</sup> AGH University of Science and Technology, al. A. Mickiewicza 30, 30-059 Krakow, Poland.

## Abstract

The demand for castings with superior properties has compelled the development and optimization of manufacturing technologies. By further developing already known techniques, we are able to contribute to the introduction of new research possibilities. The article presents the methodology of conducting simulation tests of the gravity casting process into sand moulds with the use of ablation. The ablation technique consists in spraying water through evenly spaced nozzles onto a mould into which the liquid casting alloy has been poured. The conducted research focuses on an alloy from the group of Al-Si alloys. In order to compare the effects of different techniques, additional tests were carried out for gravity casting into sand and metal die moulds. At the same time, virtual experiments were conducted to develop a simulation methodology for ablation casting technology, taking into account mould degradation. Additionally, the possibility of predicting the final mechanical properties of various manufacturing technologies was tested. Destructive tests were carried out to determine the mechanical properties in the cast samples, as well as microstructure tests and secondary dendrite spacing. The results of the mechanical tests are compared with the predicted simulation properties.

**Keywords:** casting, simulations, ablation, gravity sand casting, gravity die casting, mechanical properties

## 1. Introduction

Nowadays, the process of designing cast parts is related to computer simulation, a preliminary process before performing real experiments and included in the series of works related to the preparation of a new product manufactured using casting technology. This approach allows for the initial verification, in virtual conditions, of the correctness of the design assumptions. Computer simulations in the process of designing cast parts are already in common use. As

a design tool, they allow for the verification of design assumptions resulting from the nature of the work of the designed part. At the stage of designing the casting technology, the possibility of a preliminary evaluation by means of computer simulations helps reduce the number of real-time tests and prototypes, which allows the minimisation of costs (Abro et al., 2021; Danylchenko, 2021; Deepthi et al., 2021; Dojka et al., 2018; Tudor & Bordei, 2021). One of the methods by which subsequent design steps can be logically segregated is the Integrated System for Modelling Materials

\*Corresponding author: [marcin.malysza@kit.lukasiewicz.agh.edu.pl](mailto:marcin.malysza@kit.lukasiewicz.agh.edu.pl)

ORCID ID's: 0000-0002-7484-1393 (M. Małysza), 0000-0002-9320-0241 (S. Puzio), 0000-0003-1956-9734 (K. Major-Gabryś), 0000-0003-4925-6448 (M. Głowacki), 0000-0001-5590-0477 (D. Wilk-Kołodziejczyk), 0000-0003-4253-8725 (J. Kamińska)

© 2022 Author. This is an open access publication, which can be used, distributed and reproduced in any medium according to the Creative Commons CC-BY 4.0 License requiring that the original work has been properly cited.

and Engineering Processes (ICME). This method is used in various solutions and is described in works by Arrazola et al. (2013) and Jayal et al. (2012). This consistent approach allows the integration of computer-aided engineering design systems at different levels for design evaluation and manufacturing methods. There are many casting methods used in the industry, depending on the product planned for production. The main division is as follows: gravity casting (for permanent and non-permanent moulds) and pressure casting (low and high pressure). These methods are characterized by various parameters relating to the technology itself, as well as the materials used and alloys that can be cast (Campbell, 2003; Sobczak, 2013). The presented topic is related to the method of gravity casting into unstable forms on a sand matrix, which is exposed to water after the filling process. This method is known as ablative casting. The essence of the process consists in pouring the metal into sand moulds, which during the solidification of the casting are intensively cooled with water until complete disintegration. In this process, moulds with water-soluble binders are used (Puzio et al., 2020; United States Patent No. US 7,159,642 B2). The process is applicable to both aluminium and magnesium alloys cast in single-use moulds. Numerous authors have confirmed that the microstructure of castings made with this technology is much finer than in the case of the conventional technology of casting aluminium alloys (Ananthanarayanan et al. 1992; Dudek et al., 2014; Thompson et al., 2004). By increasing the cooling rate, both the secondary dendrite arm spacing (SDAS) and the size of the eutectic phases are reduced (Jordan, 2011; Jorstad & Rasmussen, 1997; Weiss et al. 2011). The ablation casting technology is therefore an economic process that enables the production of high-quality castings with a fine structure of dendrites and other secondary phases, characterized by an even distribution. This, in turn, improves the mechanical properties of the finished castings (Grassi & Campbell, 2010; Taghipourian et al. 2016). The ablation

casting process produces very rigid castings capable of working in cold work zones or as large aluminium structural nodes.

## 2. Methodology and materials

### 2.1. Numerical modelling

Computer simulations were carried out in Flow3D and Flow3D-Cast. A consideration of the process of physical degradation by washing with water flowing from nozzles under pressure requires a number of parameters to be taken into account. The following values of the program data should be introduced: *saturation concentration in fluid, mass transfer coefficient at dissolving surface, solid solute density, mixture density coefficient, molecular diffusion coefficient*. These parameters describe the behaviour of the sand matrix in contact with the water flowing out of the nozzles at a given speed. The computer simulations were conducted in a coupled manner. The mathematical model describing the flow phenomena is not able to take into account two liquids in one analysis. In this case, there is a liquid casting alloy that cools down and solidifies, and there is water washing the sand mould. Therefore, it was assumed to combine the results of ablation simulations, and then, based on the obtained results, another simulation should be conducted which would take into account casting and solidification. Solidification is modelled on the basis of chemical composition. The amount of microstructure components formed is predicted numerically as a function of the cooling rate. The analysis is conducted in the macro area, and it is simplified. Table 1 shows the list of compound components predicted by numerical simulation (Catalina et al. 2019; *Flow3D-Cast Manual*, 2021).

Additionally, Table 2 shows the dependence of the conditions under which the relationships included in the program database are formed.

**Table 1.** List of precipitation reactions for AlSi-based alloys

Reaction number	Reaction type	Observation
R1	$Liquid \rightarrow Al_{fcc}$	pro-eutectic
R2	$Liquid \rightarrow Al_{fcc} + Mg_2Si$	pro-eutectic
R3	$Liquid \rightarrow Al_{fcc} + Si_D$	eutectic
R4	$Liquid \rightarrow Al_{fcc} + Si_D + Mg_2Si$	eutectic
R5	$Liquid \rightarrow Al_{fcc} + Si_D + Al_3Cu_2Mg_8Si_6$	eutectic
R6	$Liquid \rightarrow Al_{fcc} + Si_D + Al_2Cu$	eutectic
R7	$Liquid \rightarrow Al_{fcc} + Si_D + Al_2Cu + Al_3Cu_2Mg_8Si_6$	eutectic

**Table 2.** Relationships for calculating the liquidus slopes in AlSi-based alloys

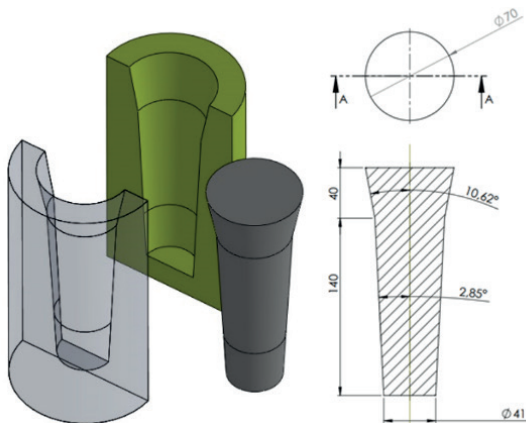
Element	Liquidus slope, $m_{li}$ [°C/wt%]
Si	$-5.584 - 0.081 \cdot Si - 9.76 e^{-4} \cdot Si^2 - 0.1169 \cdot Cu + 0.267 \cdot Mg - 0.1 \cdot Zn + 0.124 \cdot Fe$
Cu	$-2.695 + 6.574 e^{-3} \cdot Cu - 8.191 e^{-4} \cdot Cu^2$
Mg	$-4.033 - 0.088 \cdot Mg - 0.014 \cdot Cu$
Zn	$-1.449 + 0.092 \cdot Zn - 0.0395 \cdot Cu$
Fe	$-2.891 + 0.09 \cdot Fe - 0.1048 \cdot Cu$
Mn	$-1.677$

The solidification model of the liquid alloy and the change in the proportion of liquid and solid phases with a decrease in temperature is solved by the formula:

$$\rho C_p \frac{\partial T}{\partial t} = \nabla(k \nabla T) + \rho \Delta H_f \frac{\partial f_s}{\partial t} \quad (1)$$

where:  $T$  – temperature [°C];  $t$  – time [s];  $\rho$  – density [kg/m<sup>3</sup>];  $C_p$  – specific heat [J·kg<sup>-1</sup>·K<sup>-1</sup>];  $k$  – thermal conductivity [W·m<sup>-1</sup>·K<sup>-1</sup>];  $\Delta H_f$  – latent heat of fusion [J/kg];  $f_s$  – solid fraction.

Figure 1 shows an ingot and a sand mould model used in both the simulation and laboratory tests.


**Fig. 1.** Model of the ingot and the mould used in the research

The composition of the alloy used in both virtual and laboratory tests is presented in Table 3.

**Table 3.** Chemical composition of Al-Si alloy

	Si [%]	Cu [%]	Mg [%]	Mn [%]	Fe [%]	Zn [%]	Al
Ingot	7	0,15	0,35	0,25	0,15	0,25	Bal.

In accordance with the adopted methodology, the ablation simulation was carried out first, i.e. washing a sand matrix hardened with water glass and CO<sub>2</sub>. The assumed parameters allowed for the definition of the material to reflect the degradation caused by the use

of water. Figure 2 presents the stages of the decomposition of the sand form. The nozzle location, diameter and velocity of the water were set according to the laboratory trials. The sand mould definition was based on the literature regarding the saturation concentration in fluid, mass transfer coefficient at the dissolving surface, solid solute density and mixture density coefficient.

Visualization of the simulation results shows the successive stages of the mould's destruction, and the contact of water with the solidified ingot. The contact of water with the solidified aluminium alloy causes a higher cooling rate. When there is no sand barrier, it is possible to determine the heat transfer coefficient between the solidified alloy and the water.

$$Q = UA \Delta T_{LM} \quad (2)$$

where:  $Q$  – heat transfer rate, W = J/s [btu/hr];  $A$  – heat transfer surface area [m<sup>2</sup>]/[ft<sup>2</sup>];  $U$  – overall heat transfer coefficient [W/(m<sup>2</sup>·°C)]/[Btu/(hr·ft<sup>2</sup>·°F)];  $\Delta T_{LM}$  – logarithmic mean temperature difference [°C]/[°F].

Determining the value of the heat transfer coefficient is done dynamically by the solver. The calculated value is directly implemented in the next simulation, in which the casting and solidification processes are analysed. The pouring temperature in the simulation is  $T_{zai} = 700^\circ\text{C}$ , the pouring time  $t_{zai} = 2$  s. Two measuring points were used in the cavity volume of the casting mould, the first in the lower part of the cavity, and the second in the middle part. The simulation takes into account the prediction of the final mechanical properties in the volume of the ingot. Figure 3 shows a cross-section through a virtual ingot detailing the tensile strength and elongation. Additionally, the SDAS prediction is presented.

The predicted strength properties for the ablation casting process are as follows:

- tensile strength in the main area of the ingot  $R_m = 115\text{--}130$  MPa;
- elongation, in the limit  $A = 2.1\text{--}2.5\%$ ;
- SDAS dimension in the entire volume of the ingot, in the range of  $0.00058\text{--}0.00077$  m.

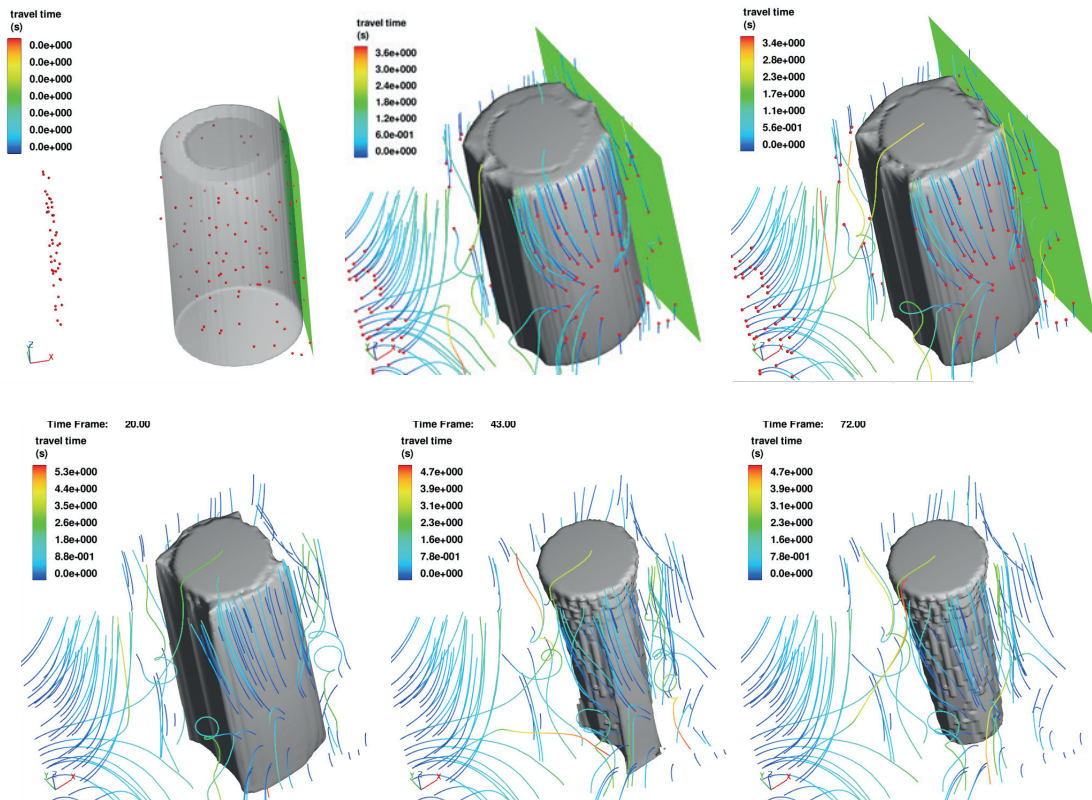


Fig. 2. Mould ablation process simulation, red dots represent flow line tracing points

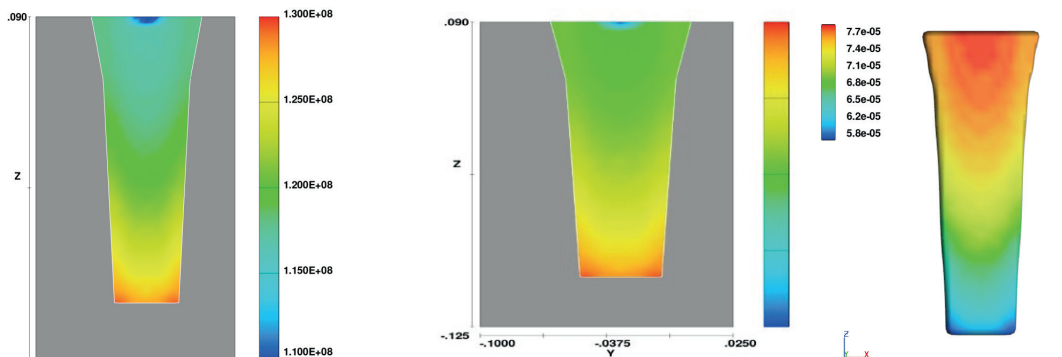


Fig. 3. Predicted strength properties in the analysed ingot and SDAS for gravity sand casting

In addition, analyses of casting and solidification in the sand mould without the use of ablation and casting into a metal mould were carried out. The boundary conditions are the same as for the ablation simulation. Figure 4 shows the forecast of mechanical properties for this casting method.

The predicted strength properties for the ablation casting process are as follows:

- tensile strength in the main area of the ingot  $R_m = 155\text{--}170$  MPa;
- elongation, in the limit  $A = 5.5\text{--}6\%$ ;
- SDAS dimension in the entire volume of the ingot, in the range of  $0.0005\text{--}0.00058$  m.

Another variant involves casting into a metal mould. The casting conditions were the same as in the previous variant. Defined die material is steel H-13, the die mould temperature  $T_D = 200^\circ\text{C}$ . Figure 5 shows the forecast of mechanical properties for this casting method.

The predicted strength properties for the ablation casting process are as follows:

- tensile strength in the main area of the ingot  $R_m = 157\text{--}180$  MPa;
- elongation, in the limit  $A = 3.25\text{--}5.5\%$ ;
- SDAS dimension in the entire volume of the ingot, in the range of  $0.00012\text{--}0.00029$  m.

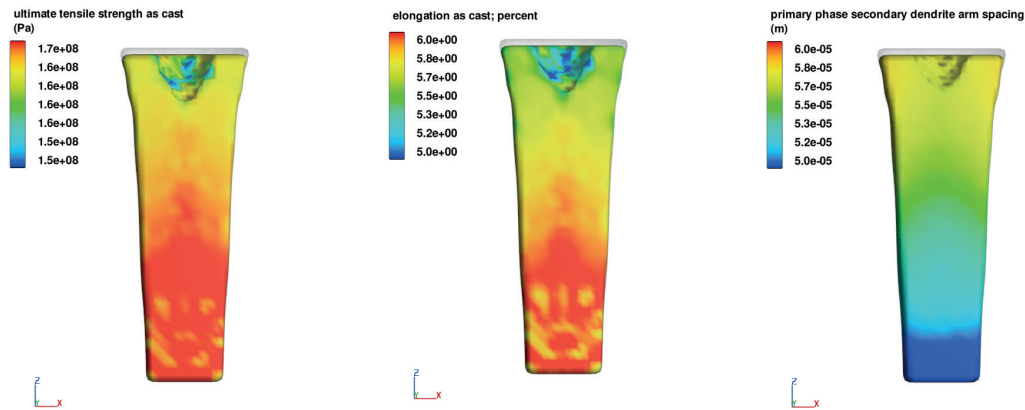


Fig. 4. Projected strength properties in the analysed ingot and SDAS for ablation process

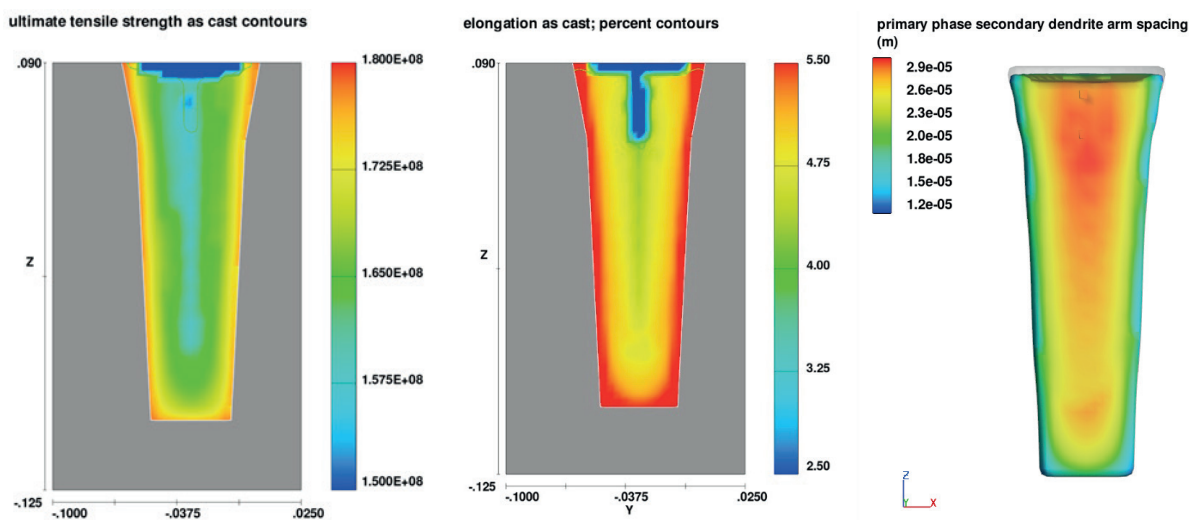


Fig. 5. Projected strength properties in the analysed ingot and SDAS for gravity die casting

## 2.2. Laboratory trials

The melt in the ablation casting technology was made using a device for removing moulding sand from castings and subsequent cooling. The equipment is located at the Łukasiewicz – Krakow Institute of Technology, formerly known as the Foundry Research Institute, and is protected by the Polish patent number P.404518. The diagram of this device is shown in Figure 6.

The method of operation of the device is as follows: The mould (14) is placed on the work table (2) and extended outside the chamber (1). After flooding, it is placed in the chamber (1). The working table (2), lowering it, introduces the form (14) into the zone of the ablative medium (water) (5). The mould is broken and the casting is cooled down. A mixture of moulding sand and water flows into the tank (6). After breaking the mould (14), the work table (2) extends beyond the chamber (1) and the finished, cooled casting can be removed.

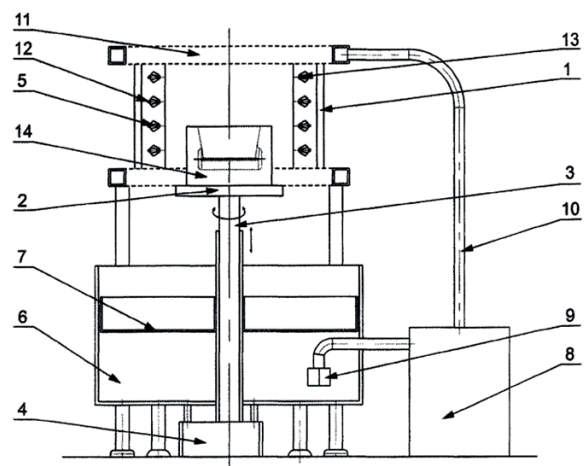


Fig. 6. Diagram of the device for removing moulding sand from a casting and its cooling; where: 1 – chamber; 2 – mobile working table; 3 – lift; 4 – drive system; 5 – nozzles; 6 – tank for flowing liquid cooling medium; 7 – basket for collecting sand from a broken mould; 8 – pump; 9 – filter; 10 – high-pressure hoses for supplying liquid cooling medium to nozzles; 11 – distribution bar; 12 – joints; 13 – deflectors; 14 – mould

The test castings were made of an aluminium-silicon alloy (AlSi7Mg). The melts were carried out simultaneously in a sand form, a die and in a sand form using the ablation casting technology (Figs. 7–9). Thermocouples were attached to each mould, thanks to which temperature measurements were taken on three levels of the moulds during the process (in the

upper part of the casting, in the middle and in the lower part). The test castings were made in moulds made on the basis of a microwave-hardened geopolymeric binder.

The composition of the mass was as follows:

- medium quartz sand – 100 parts by weight,
- geopolymer binder – 1 part by weight.

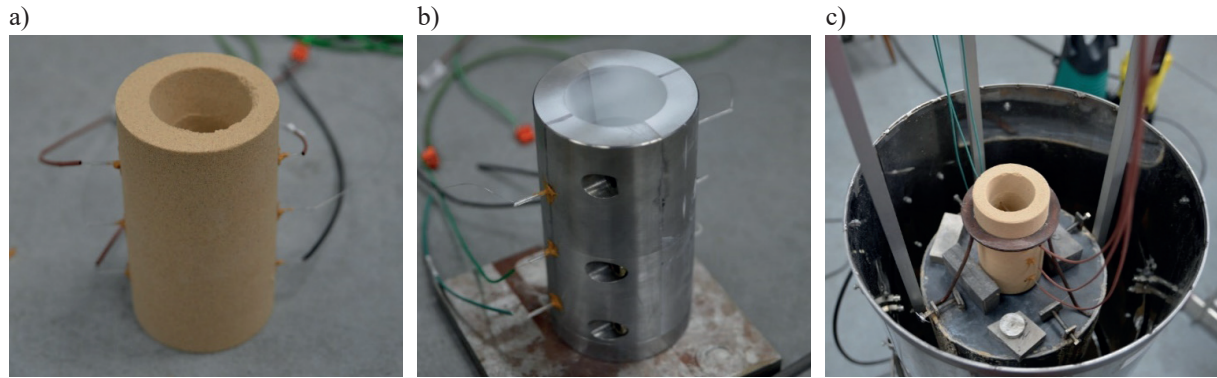


**Fig. 7.** Moulds prepared for pouring with a liquid alloy: a) sand; b) metal; c) sand on the ablation casting station

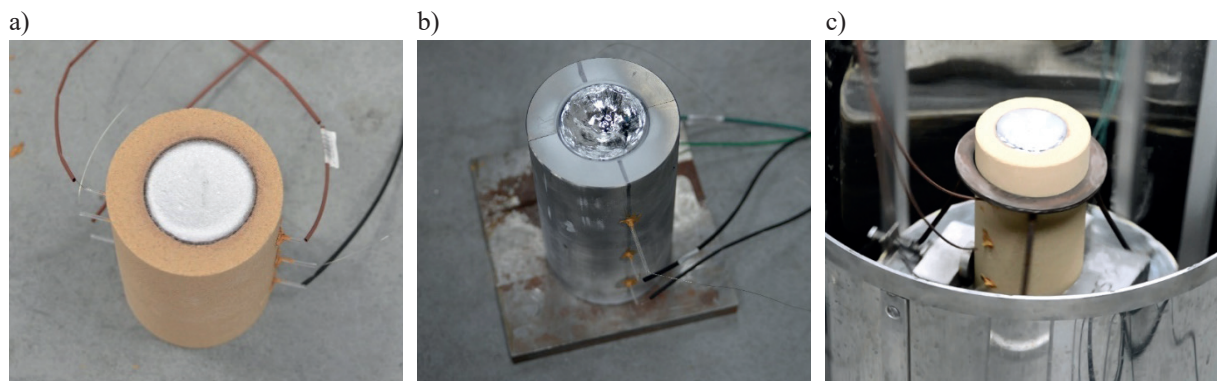


**Fig. 8.** Moulds flooded with a liquid alloy: a) sand mould intended for classic cooling at ambient temperatures; b) die; c) sand mould on ablation casting station

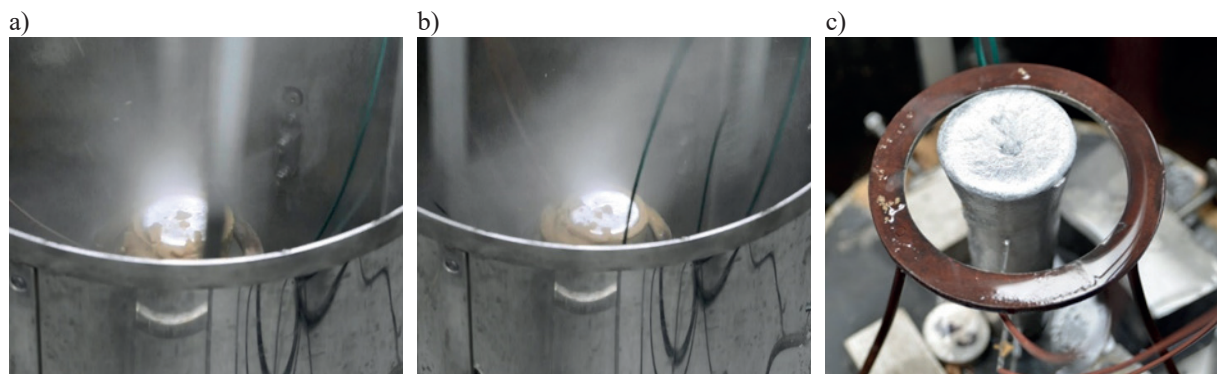


**Fig. 9.** Ablative casting process mould during ablative cooling and smashing (a, b) and finished chilled casting (c)

The thermal analysis was carried out using two measuring devices: for traditional casting, the curves were recorded using a multichannel MrAC-15 recorder, and for ablation casting, the TES 1384 recorder was used

from the moment it was flooded with the liquid alloy. A shorter time was not enough for the casting to keep the proper shape, and a longer time did not guarantee changes in the microstructure of the castings (Fig. 10).

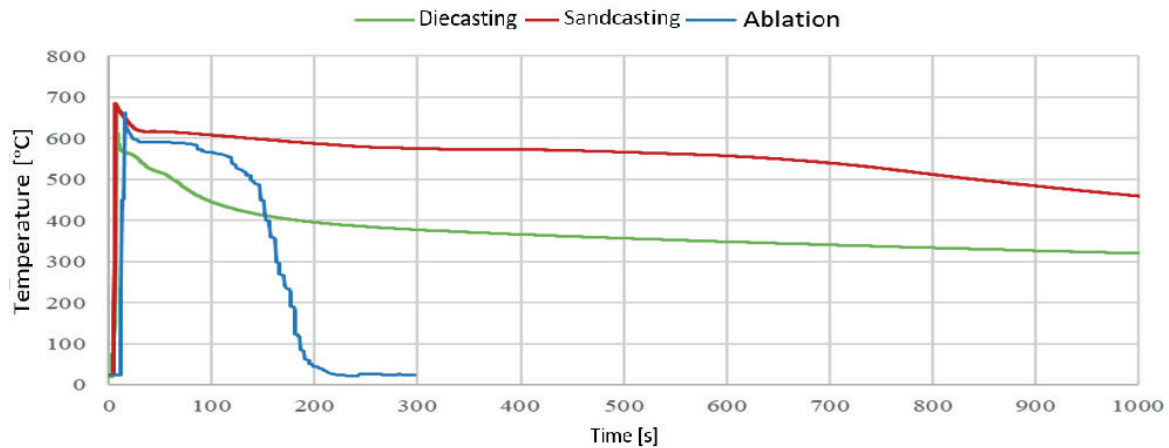


**Fig. 10.** Summary of cooling curves (average for three levels) for each of the presented technologies

The ablation cast reached room temperature in no more than 200 s. Samples for microstructure tests were made from ready castings, analogically at three levels of castings and for strength tests. In order to perform microstructure tests allowing for the assessment of differences on three levels of the casting, samples were cut out from each of them. The specimens were first polished on a Struers polisher, on 220, 500 and 1000 papers with 9, 3, 1 and 1/4 micron diamond pastes, and then etched in a 1% HF solution in distilled water. The observations were made on a Zeiss light microscope with the AxioObserver Zm10 program. The shoulder distance of the second-order dendrites, SDAS, was observed at 50 $\times$  magnification on the digested samples by the 10 oriented secant method. The dispersion of the dendritic structure in each of the tested castings for the middle level is shown in Figure 11.

**Table 4.** Distance of 2<sup>nd</sup> order dendrite arms [ $\mu\text{m}$ ], area 50 $\times$

Form	Place in industry			
	down	middle	bottom	average
Ablation	36.1	45.8	36.3	39.4
Sand	56.6	74.5	85.5	72.2
Die	33.5	41.2	42.1	38.9

The observations showed that there was a differentiation in the dispersion of the dendritic structure between the tested castings, reflecting the differences in the cooling rate. Based on the cooling rate, which is high for die casting and low for sand casting, the ablation technique gives a middle point for that parameter. The cooling rate has an impact on grain size, which is presented in Figure 11a and c.

The grain size mainly corresponds with the mechanical properties. Finer grain size gives higher mechanical properties. However, no changes were observed between the different zones of each casting. The static tensile test at ambient temperature was carried out in accordance with PN-EN ISO 6892-1:2016-09: *Metals – Tensile test – Part 1: Test method at room temperature (section Method B)*. A testing machine of EU-20 type, serial number 990.55/88.7 with a maximum range of 200 kN was used for the tests. The stress velocity increase was 15.9 MPa/s. Classic standardized samples were used in the research. The results of strength tests for castings made in the ablation casting technology were compared with die and sand casting and are presented in Table 5.

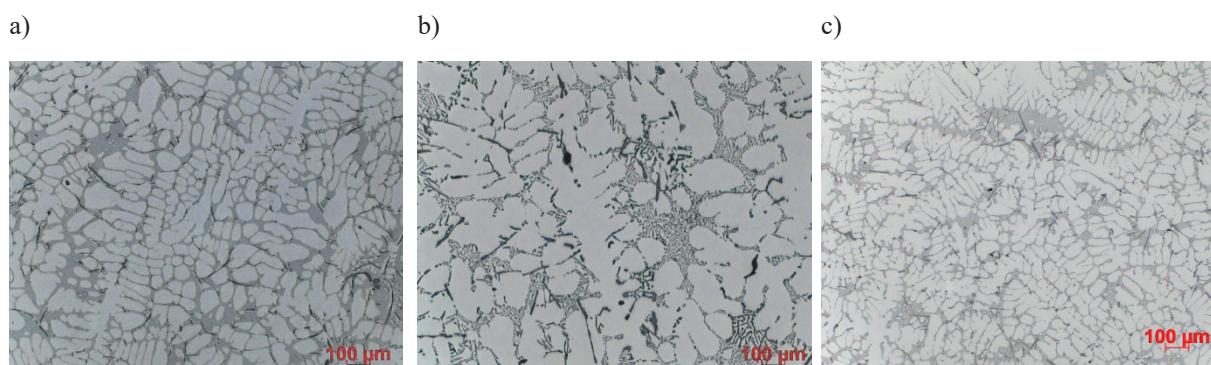


**Fig. 11.** Dendritic structure dispersion, centre, LM, grasses (HF, micron area 100 $\times$ ): a) ablation; b) sand; c) die

The major reason for proposing the use of such a technology for ablation casting is the possibility of using complicated geometries of moulds and cores due to the use of 3D printed sand moulds. The complexity of die mould is limited to the possibility of opening

of the two die halves, and the archived properties for ablation casting compared to die casting makes it an interesting technology for more industrial applications

In Figure 12, the comparison of the real ablation and in the virtual experiment is presented.

**Table 5.** Results of the casting strength tests

No.	Sample designation	$d_o$ [mm]	$S_0$ [mm <sup>2</sup> ]	$L_0$ [mm]	$F_{p0.2}$ [kN]	$YS_{0.2}$ [MPa]	$F_m$ [kN]	$UTS$ [MPa]	$L_u$ [mm]	Elongation [%]	$d_u$ [mm]	Neck [%]
geopol, microwave curing												
1.	sand	4.99	19.6	15	1.90	97.0	2.1	109	15.06	0.4	4.97	0.8
2.	die	5.02	19.8	15	2.65	133.5	3.5	175	15.49	3.3	4.95	2.8
3.	ablation	5.00	19.6	15	2.80	143.0	3.4	172	15.41	2.7	4.93	2.6

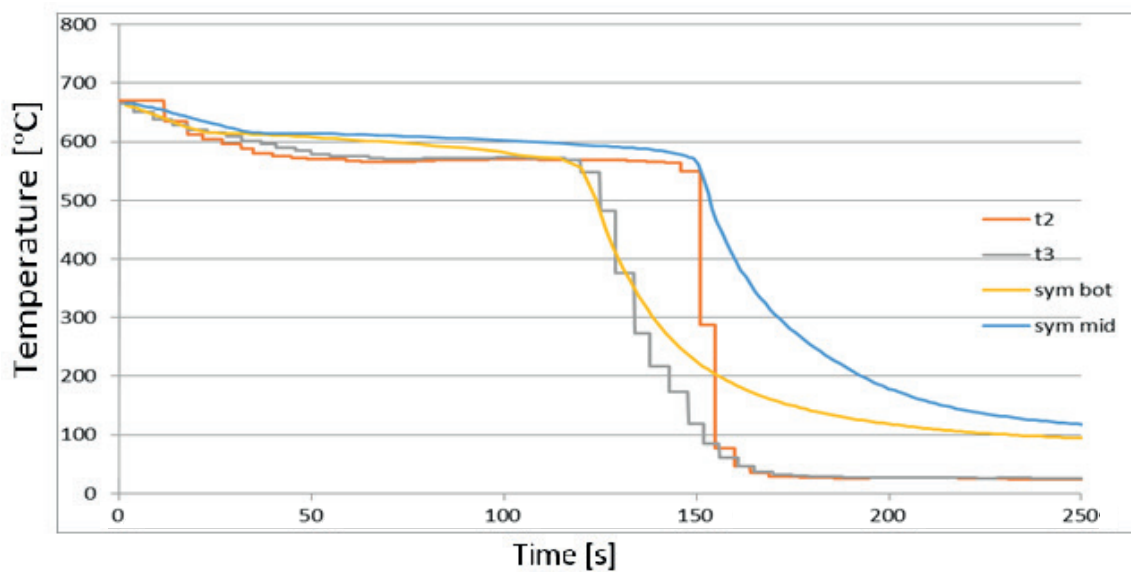


**Fig. 12.** Comparison of solidification curves for the real ablation process and in the virtual experiment

Both the simulation and the real experiment had a good degree of accuracy. The solidification process in the first phase was very similar and the point of quick cooling was also very close between the two. The main crystallization and creation of microstructure occurred between 680°C and 550°C. In that temperature range, the curves of the simulation and the real laboratory trial converged.

### 3. Discussion and conclusions

The conducted laboratory tests allowed the determination of the material properties of the castings obtained under various technological conditions. Furthermore, computer simulations were carried out which took the boundary conditions resulting from the specificity of each casting technology into account. The comparison

of the simulation results and laboratory tests allowed the assessment of whether the model used in the simulation would be scalable and used for the design of castings made by the ablative method. A mechanical properties prediction module was used in the program. Tables 6 and 7 present a summary of the basic mechanical properties and the distance between the arms of the second-order dendrites obtained from the simulation and the laboratory tests.

**Table 6.** Comparison of simulation results and conducted laboratory tests

Name	Cast- $R_m$ [MPa]	Cast- $A$ [%]	Sim- $R_m$ [MPa]	Sim- $A$ [%]
Sand	109	0.4	130	2
Die	175	3.3	165	4
Ablation	172	2.7	170	5.5

**Table 7.** Dendrite arm spacing

	Area of the casting				Simulation			
	bottom	middle	top	avg.	bottom	middle	top	avg.
Ablation	36.1	45.8	36.3	39.4	45	50	55	50
Sand	56.6	74.5	85.5	72.2	58	71	77	68.6
Die	33.5	41.2	42.1	38.9	25	29	33	29

The predicted mechanical properties under simulated conditions differ slightly in terms of tensile strength. The differences in sand casting, die casting, and ablation casting successively are 19%, 6%, 2%. The biggest difference in strength prediction was observed for sand casting. Significant discrepancies were weighed in the prediction of elongation. For sand casting, the difference is 4 times, for die casting it is 20%, while for ablative casting, the difference is 2 times. The prediction of dendrite growth was also compared. In this case, the mean value depending on the height is 25%, 5%, 26%, respectively. The most similar results were obtained in the middle area of the ingot.

The differences between the laboratory tests and the simulation results may be due to the defined database of the Flow3D program. The phases that are described in Table 1 show the precipitation reactions of

Al-Si. There is a possibility that the numerical model does not take into account all of the phase transformations in comparison to the real casting process and solidification. Depending on the defined chemical composition, the program numerically determines the number of microstructure components being formed. For the solidification conditions occurring in the metal mould, and where the results are very similar, the removal of temperature from the ingot volume is uniform, unlike in the sand mould where the solidification is prolonged and accelerated in the case of ablation casting.

The numerical model and the research carried out allow us to conclude that it is possible to use a computer program to simulate more complex parts in ablation casting technology. Additional simulations are required to correct the parameters related to the prediction of strength properties, especially elongation.

## References

- Abro, S.H., Shamsi, H.A., Wahab, S., & Mohsin, A. (2021). Design and development of casting part by simulation. *International Conference on Energy, Water and Environment – ICEWE-2021. New Campus, University of Engineering and Technology Lahore, 31<sup>st</sup> March 2021, Lahore, Pakistan* (pp. 452–457). <https://conferences.uet.edu.pk/icewe/2021/book-of-abstracts/>.
- Ananthanarayanan, L., Samuel, F.H., & Gruzelski, J. (1992). Thermal analysis studies of the effect of cooling rate on the microstructure of 319 aluminium alloy. *AFS Transactions*, 100, 383–391.
- Arrazola, P.J., Özel, T., Umbrello, D., Davies, M., & Jawahir, I.S. (2013). Recent advances in modelling of metal machining processes. *CIRP Annals*, 62(2), 695–71. <https://doi.org/10.1016/j.cirp.2013.05.006>.
- Campbell, J. (2003). *Castings*. Second edition, Butterworth Heinemann.
- Catalina, A.V., Xue, L., & Monroe, C.A. (2019). A solidification model with application to AlSi-based alloys. In M. Tiryakioglu, W. Griffiths, M. Jolly (Eds.), *Shape Casting. 7<sup>th</sup> International Symposium Celebrating Prof. John Campbell's 80<sup>th</sup> Birthday* (pp. 201–213), Springer Cham.
- Danylchenko, L. (2021). Comparative analysis of computer systems for casting processes simulation. In *International Conference Advanced Applied Energy and Information Technologies 2021* (pp. 105–113). Retrieved October 21, 2022, [http://elartu.tntu.edu.ua/bitstream/lib/36933/2/ICAAEIT\\_2021\\_Danylchenko\\_L-Comparative\\_analysis\\_105-113.pdf](http://elartu.tntu.edu.ua/bitstream/lib/36933/2/ICAAEIT_2021_Danylchenko_L-Comparative_analysis_105-113.pdf).
- Deepthi, T., Balamurugan, K., & Uthayakumar, M. (2021). Simulation and experimental analysis on cast metal runs behaviour rate at different gating models. *International Journal of Engineering Systems Modelling and Simulation*, 12(2–3), 156–164. <https://doi.org/10.1504/IJESMS.2021.10038002>.
- Dojka, R., Jezierski, J., & Campbell, J. (2018). Optimized gating system for steel castings. *Journal of Materials Engineering and Performance*, 27(10), 5152–5163. <https://doi.org/10.1007/s11665-018-3497-1>.
- Dudek, P., Fajkiel, A., Reguła, T., & Bochenek, J. (2014). Research on the technology of ablation casting of aluminum alloys / Badania nad technologią odlewania ablacyjnego stopów aluminium. *Transactions of Foundry Research Institute / Prace Instytutu Odlewnictwa*, LIV(2), 23–35.
- Flow3D-Cast Manual* (2021).
- Grassi, J., Campbell, J., Hartlieb, M., & Major, F. (2009). The ablation casting process. *Materials Science Forum*, 618–619, 591–594. <https://doi.org/10.4028/www.scientific.net/MSF.618-619.591>.
- Jayal, A.D., Badurdeen, F., Dillon, O.W., Jr, & Jawahir, I.S. (2012). Sustainable manufacturing: Modeling and optimization challenges at the product, process and system. In G.J. Schmitz, U. Pahl (Eds.), *Integrative Computational Materials Engineering. Concepts and Applications* (pp. 144–152), John Wiley & Sons.

- Jordon, L.W.J.B. (2011). Monotonic and cyclic characterization of five different casting process on a common magnesium alloy. In *ASME 2011 International Manufacturing Science and Engineering Conference. Volume 1* (pp. 7–16). <https://doi.org/10.1115/MSEC2011-50173>.
- Jorstad, J.L., Rasmussen, W.M., & Zalensas, D.L. (2001). *Aluminum Casting Technology*. 2<sup>nd</sup> ed., American Foundry Society.
- Puzio, S., Kamińska, J., Angrecki, M., & Major-Gabryś, K. (2020). Effect of the type of inorganic binder on the properties of microwave-hardened moulding sands for ablation casting technology. *Archives of Metallurgy and Materials*, 65(4), 1385–1390. <https://doi.org/10.24425/amm.2020.133704>.
- Taghipourian, M., Mohammadaliha, M., Boutorabi, S., & Mirdamadi, S. (2016). The effect of waterjet beginning time on the microstructure and mechanical properties of A356 aluminum alloy during the ablation casting process. *Journal of Materials Processing Technology*, 238, 89–95. <https://doi.org/10.1016/j.jmatprotec.2016.05.004>.
- Thompson, S., Cockcroft, L.M., & Wells, M.M. (2004). Advanced high metals casting development solidification of aluminium alloy A356. *Materials Science and Technology*, 20, 194–200. <https://doi.org/10.1179/026708304225011199>.
- Tudor, B.D., & Bordei, M. (2021). The applying software programs, for technological design, and simulation of the casting process, in optimizing the technology of making castings. *Journal of Physics: Conference Series*, 1960, 012002.
- Sobczak, J.J. (red.) (2013). *Poradnik odlewnika*. Wydawnictwo Stowarzyszenia Technicznego Odlewników Polskich.
- United States Patent No. US 7,159,642 B2.
- Weiss, D., Grassi, J., Schultz, B., & Rohatgi, P. (2011). Ablation of hybrid metal matrix composites. *Transactions of American Foundry Society*, 119, 35–42.